Lawrence Berkeley National Laboratory

Lawrence Berkeley National Laboratory

Title

Molecular environmental science using synchrotron radiation: Chemistry and physics of waste
form materials

Permalink

https://escholarship.org/uc/item/7249r0qk

Authors

Lindle, Dennis W.
Shuh, David K.

Publication Date

2005-02-28

eScholarship.org Powered by the California Digital Library
University of California

Molecular Environmental Science Using Synchrotron Radiation: Chemistry and Physics of Waste Form Materials*

EPSCoR Partnership Award: DE-FG02-01ER45898
FY2002 Progress Report (Oct. 2001-Sept. 2002)

Dennis W. Lindle
Department of Chemistry
University of Nevada Las Vegas
Las Vegas, NV 89154-4003 USA

David K. Shuh
Actinide Chemistry Group
Chemical Sciences Division
Lawrence Berkeley National Laboratory
MS 70A-1150, One Cyclotron Road
Berkeley, CA 94720 USA

* This work was supported by the Nevada Department of Energy EPSCoR State-National Laboratory Partnership program under Grant No. DE-FG02-01ER45898.

28 February 2003

Molecular Environmental Science Using Synchrotron Radiation: Chemistry and Physics of Waste-Form Materials

FY2002 Progress Report (Oct. 2001-Sept. 2002)

Table of Contents

I. Executive Summary 3
II. Progress Report for FY2002 5
Pyrochlore Ceramics 5
Glasses 10
Beamline Development 12
Summary 12
Scientific Activities 13
III. References 15

Molecular Environmental Science Using Synchrotron Radiation: Chemistry and Physics of Waste Form Materials

FY2002 Progress Report (Oct. 2001-Sept. 2002)

I. Executive Summary

Production of defense-related nuclear materials has generated large volumes of complex chemical wastes containing a mixture of radionuclides. The disposition of these wastes requires conversion of the liquid and solid-phase components into durable, solid forms suitable for long-term immobilization [1]. Specially formulated glass compositions and ceramics such as pyrochlores and apatites are the main recipients for these wastes. The performance of these waste-form materials is largely determined by the loading capacity for the waste constituents (radioactive and non-radioactive) and the resultant chemical and radiation resistance of the waste-form package to leaching (durability). An important consideration linked to the durability of waste-form materials is the local structure around the waste components. Equally important is the local structure of constituents of the glass and ceramic host matrix. Knowledge of the structure in the waste-form host matrices is essential, prior to and subsequent to waste incorporation, to evaluate and develop improved waste-form compositions based on scientific considerations. Structural information also provides a mechanistic basis to understand properties underlying durability.

The soft-x-ray synchrotron-radiation-based technique of near-edge x-ray-absorption fine structure (NEXAFS) is a unique method for investigating oxidation states and structures of low-Z elemental constituents forming the backbones of glass and ceramic host matrices for waste-form materials. While nuclear magnetic resonance (NMR) is primarily employed to obtain speciation information from low-Z elements in waste forms (primarily glasses), it is incompatible with metallic impurities contained in real waste and is thus limited to studies of idealized model systems. Furthermore, light metal ions in ceramic hosts, such as titanium, are also ideal for investigation by NEXAFS in the soft-x-ray region. Thus, one of our main objectives is to understand outstanding issues in waste-form science via NEXAFS investigations and to translate this understanding into better waste-form materials, followed by eventual capability to investigate "real" waste-form materials by the same methodology. We have conducted several detailed structural investigations of both pyrochlore ceramic and borosilicate-glass materials during the reporting period and developed improved capabilities at Beamline 6.3.1 of the Advanced Light Source (ALS) to perform the studies.

The use of ceramic pyrochlores as host matrices for actinide-rich wastes is receiving increased attention since recent experimental discoveries showed the isovalent substitution of Zr for Ti in $Gd_2Ti_2O_7$ results in an increase of 4 to 5 orders of magnitude in resistance to energetic particle irradiation. Cation disorder and the accompanying anion Frenkel defects are the main cause for the dramatic increase in oxide-ion conductivity and radiation tolerance in ordered pyrochlore-structured oxide materials [2]. Several experimental and theoretical investigations have been carried out to understand the mechanism responsible for the cation antisite disorder and the accompanying anion Frenkel defects. There is limited direct experimental evidence for the presence of cation antisite disorder in what should normally be a highly ordered pyrochlore structure [3]. We have performed titanium-2*p* and oxygen-1*s* NEXAFS and x-ray photoelectron spectroscopy (XPS) investigations to elucidate the mechanism leading to cation antisite disorder and anion Frenkel defects. These studies show the Ti^{4+} ions in $Gd_2Ti_2O_7$ pyrochlore occupy octahedral sites with a tetragonal distortion induced by the vacant 8*a* oxygen sites located in the *ab* plane adjacent to TiO_6 octahedra. The coordination of Zr increases from 6 to nearly 8 with

increasing substitution of Zr for Ti in $Gd_2(Ti_{1-y}Zr_y)_2O_7$. To compensate for the increased coordination of Zr, oxygen anions migrate either from occupied 48*f* or 8*b* sites to vacant 8*a* sites.

The mechanism and structural properties leading to superior radiation resistance [4] of these same pyrochlore materials also has been characterized. Ion-beam irradiation of an increasingly Zr-substituted series of pyrochlores has been studied by NEXAFS and XPS to yield detailed structural information. A phase transformation occurs from the ordered pyrochlore structure (*Fd*3*m*) to the defect fluorite structure (*Fm*3*m*) following 2.0 MeV Au^{2+} ion-beam irradiation of $Gd_2(Ti_{1-y}Zr_y)_2O_7$, irrespective of the Zr concentration. Irradiated $Gd_2(Ti_{1-y}Zr_y)_2O_7$ samples with $y \leq 0.5$ are amorphous although they have significant short-range ordering. In contrast, sample compositions with $y \geq 0.75$ retain their crystallinity after ion-beam irradiation. The structures of Zr^{4+} in the irradiated $Gd_2(Ti_{1-y}Zr_y)_2O_7$ with $y \geq 0.75$ are almost the same as in cubic fluorite-structured yttria-stabilized zirconia (y-ZrO_2), providing solid evidence for phase transformation. The rearrangements of oxygen anions among 48*f*, 8*b*, and 8*a* sites, and of cations between 16*c* and 16*d* sites in ordered $Gd_2Ti_2O_7$ requires more energy compared to the relatively less-ordered pyrochlore-structured $Gd_2Zr_2O_7$. Thus, during phase transformation induced by ion-beam irradiation, $Gd_2(Ti_{1-y}Zr_y)_2O_7$ samples with $y \leq 0.5$ become amorphous, whereas compositions with $y \geq 0.75$ retain crystalline structure. The XPS data show a single narrow peak at 529.6 eV with FWHM of ~1.5 eV characteristic of surface Ti-O (48*f*) in $Gd_2Ti_2O_7$.

The speciation of radionuclide constituents in glass waste forms and the interactions of the low-Z glass constituents (boron, oxygen, and sodium) comprising (and defining) the basic properties of the glass network are particularly critical in determining long-term durability [5-7]. The focus of boron studies in glasses is to determine the amount of three-coordinate $[BO_3]^{3-}$ relative to four-coordinate $[BO_4]^{5-}$ species in several glass formulations. Several theories of glass durability (*i.e.,* chemical and physical resistance to leaching by water) focus on the coordination of boron as a key aspect yet to be understood. We have pursued this effort by measuring and determining boron coordination in several glass series and reference materials. Currently, the results from our boron studies are being correlated to results from NMR (where possible) and to leaching studies. In particular, we have used boron *K*-edge NEXAFS to determine the coordination for several well-known base (RD series) and Hf glass series (Hf used as a surrogate for tetravalent actinides) from PNNL. Similar to the boron investigations, we have continued to perform extended x-ray-absorption fine-structure (EXAFS) measurements of waste-form glass and reference materials at the sodium *K* edge. We finalized the data collection from two series of glasses, including the Hf glass series mentioned above, at two temperatures along with an improved set of sodium reference materials. Inspection of the EXAFS data indicates sodium coordination in the Hf glasses is similar, with no significant differences as hafnium concentration increases. The EXAFS results also suggest oxygen is the nearest neighbor with silicon atoms in the second shell, although the second shell could be fit nearly as well as a mixed shell of silicon and aluminum atoms.

Most of the experimental investigations have been performed at Beamline 6.3.1 of the ALS. Beamline 6.3.1, an entrance-slitless bend-magnet beamline, operates from 200 eV to 2000 eV with a Hettrick-Underwood varied-line-space (VLS) grating monochromator. To perform the NEXAFS studies of waste-form materials, an improved beam-intensity monitor (I_0) system was implemented, a fluorescence-detector system was installed, and a low-temperature sample-stage capability was developed. Furthermore, extensive characterization and optimization of the optical properties of the beamline was conducted to permit state-of-the-art NEXAFS measurements.

Molecular Environmental Science Using Synchrotron Radiation: Chemistry and Physics of Waste Form Materials

II. Progress Report for FY2002

Production of defense-related nuclear materials has generated large volumes of complex chemical wastes containing a mixture of radionuclides. The disposition of these wastes requires conversion of the liquid and solid-phase components into durable, solid forms suitable for long-term immobilization [1]. Specially formulated glass compositions, many of which have been derived from glass developed for commercial purposes, and ceramics such as pyrochlores and apatites, will be the main recipients for these wastes. The performance characteristics of waste-form glasses and ceramics are largely determined by the loading capacity for the waste constituents (radioactive and non-radioactive) and the resultant chemical and radiation resistance of the waste-form package to leaching (durability).

There are unique opportunities for the use of near-edge soft-x-ray absorption fine structure (NEXAFS) spectroscopy to investigate speciation of low-Z elements forming the backbone of waste-form glasses and ceramics. Although nuclear magnetic resonance (NMR) is the primary technique employed to obtain speciation information from low-Z elements in waste forms, NMR is incompatible with the metallic impurities contained in real waste and is thus limited to studies of idealized model systems. In contrast, NEXAFS can yield element-specific speciation information from glass constituents without sensitivity to paramagnetic species. Development and use of NEXAFS for eventual studies of real waste glasses has significant implications, especially for the low-Z elements comprising glass matrices [5-7]. The NEXAFS measurements were performed at Beamline 6.3.1, an entrance-slitless bend-magnet beamline operating from 200 eV to 2000 eV with a Hettrick-Underwood varied-line-space (VLS) grating monochromator, of the Advanced Light Source (ALS) at LBNL. Complete characterization and optimization of this beamline was conducted to enable high-performance measurements.

Waste-Form Pyrochlore Ceramics

The use of pyrochlores as host matrices for actinide-rich wastes is receiving increased attention because recent experimental discoveries have shown isovalent substitution of Zr for Ti in $Gd_2Ti_2O_7$ results in an increase of 4 to 5 orders of magnitude in resistance to energetic particle irradiation [2]. Cation disorder and the accompanying anion Frenkel defects are the main cause for the dramatic increase in oxide-ion conductivity and radiation tolerance in ordered pyrochlore-structured oxide materials [2,8]. Several experimental and theoretical investigations have been carried out to understand the mechanism responsible for the cation antisite disorder and the accompanying anion Frenkel defects. There is limited direct experimental evidence for the presence of cation antisite disorder in what should normally be a highly ordered pyrochlore structure [3]. The results from our waste-form pyrochlore research investigations are being prepared for publication and several are close to submission [9-11].

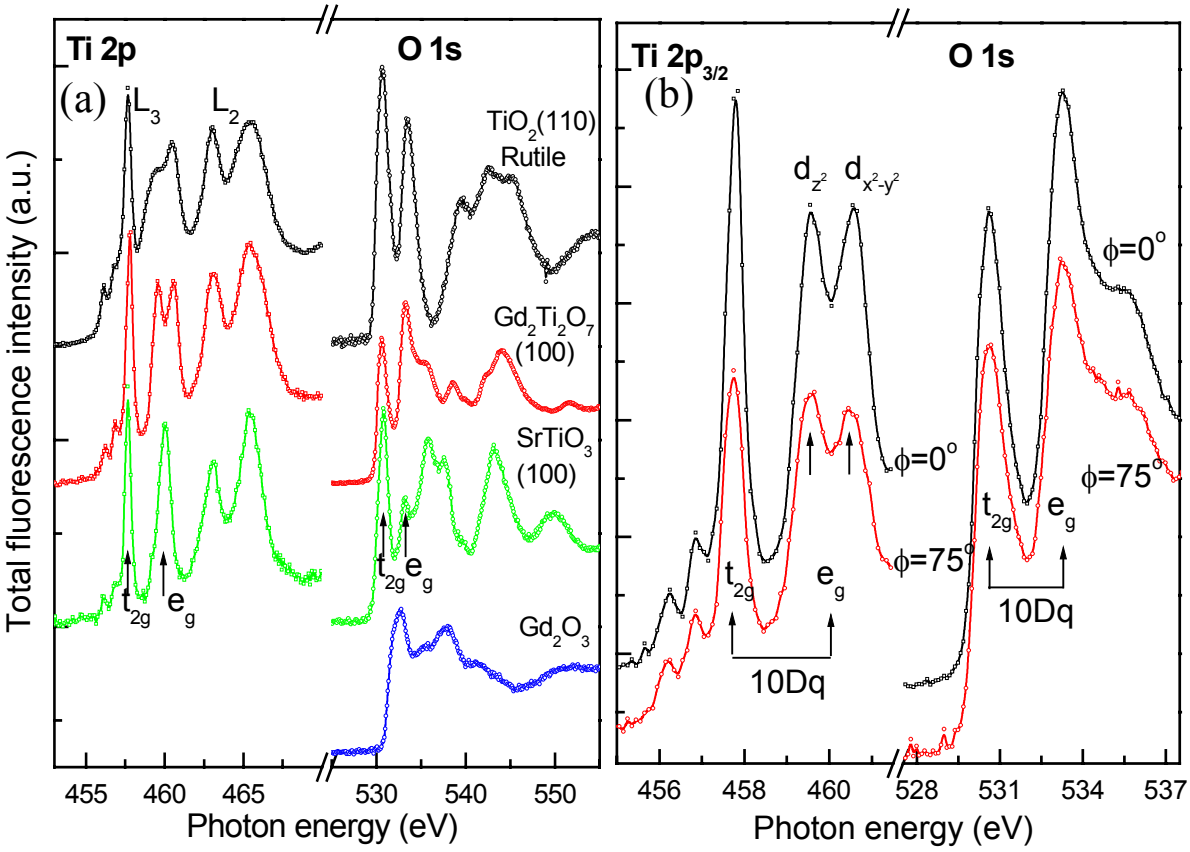

Fig. 1. (a) Normal incidence (ϕ=0°) Ti-2*p* and O-1*s* NEXAFS of TiO_2(110) (rutile), $Gd_2Ti_2O_7$(100), $SrTiO_3$(100), and Gd_2O_3. (b) Polarized Ti-2$p_{3/2}$ and O-1*s* NEXAFS recorded at normal and gracing x-ray incidence angles (ϕ) for single-crystal $Gd_2Ti_2O_7$.

Normal incidence (ϕ=0°) Ti-2*p* and O-1*s* NEXAFS spectra of TiO_2(110) (rutile), $Gd_2Ti_2O_7$(100), $SrTiO_3$(100), and Gd_2O_3 are shown in Fig. 1(a). The features labeled L_3 and L_2 for TiO_2, $Gd_2Ti_2O_7$, and $SrTiO_3$ predominantly result from transitions to the final states Ti^{4+}: $(2p_{3/2,1/2})^{-1}$ $3d^1$ - O^{2-}: $2p^6$, where $(2p_{3/2,1/2})^{-1}$ denotes a hole in the $2p_{3/2}$ or $2p_{1/2}$ state. The t_{2g} and e_g features result from transitions to the final states Ti^{4+}: $(2p_{3/2})^{-1}3d(2t_{2g})^1$ - O^{2-}: $2p^6$ and Ti^{4+}: $(2p_{3/2})^{-1}$ $3d(3e_g)^1$ - O^{2-}: $2p^6$, respectively. The energy separations between the t_{2g} and e_g states, which are related to the crystal-field strength, are 2.2 eV, 2.3 eV, and 2.4 eV for TiO_2, $Gd_2Ti_2O_7$, and $SrTiO_3$, respectively. Comparison of Ti-2*p* NEXAFS for $Gd_2Ti_2O_7$, TiO_2, and $SrTiO_3$ suggests Ti in $Gd_2Ti_2O_7$ is tetravalent and occupies sites of octahedral symmetry. In addition, the e_g states, which consist of atomic d_{z^2} and $d_{x^2-y^2}$ orbitals, are directed towards ligand anions and are therefore much more sensitive to deviations from octahedral symmetry of Ti. Consequently, the splitting of e_g states into d_{z^2} and $d_{x^2-y^2}$ for $Gd_2Ti_2O_7$, as in TiO_2, but unlike in $SrTiO_3$ where Ti occupies perfect octahedral symmetry, suggests Ti in $Gd_2Ti_2O_7$ occupies sites with distorted octahedral symmetry. The energy separations between the d_{z^2} and $d_{x^2-y^2}$ orbitals is 1.0 eV and 1.2 eV for $Gd_2Ti_2O_7$ and TiO_2, respectively, and results from (and is a measure of) the degree of

distortion from pure octahedral symmetry. Comparison of O-1*s* NEXAFS of $Gd_2Ti_2O_7$ with TiO_2, $SrTiO_3$, and Gd_2O_3 suggests the oxygen anions coordinated to Gd^{3+} also contribute spectral intensity in the vicinity of the e_g states derived from the TiO_6 octahedra in $Gd_2Ti_2O_7$.

Polarized Ti-2$p_{3/2}$ and O-1*s* NEXAFS recorded at different incidence angles (ϕ) for single-crystal $Gd_2Ti_2O_7$ are shown in Fig. 1(b). The polarization-dependent Ti-2*p* and O-1*s* NEXAFS reflect weaker covalence between Ti(d_{z^2}) and O(p_z) along the *c* axis with an elongated Ti-O distance suggesting a tetragonal distortion of TiO_6 octahedra in $Gd_2Ti_2O_7$, as in TiO_2. This supports the notion the e_g states, which are projected directly towards oxygen anions, split into lower-energy d_{z^2} and higher-energy $d_{x^2-y^2}$ states, unlike the t_{2g} states. In addition, these results show the vacant 8*a* oxygen sites are located in the *ab* plane adjacent to TiO_6 octahedra in $Gd_2Ti_2O_7$, inducing tetragonal distortion. Two additional transitions at 532.2 eV and 534.9 eV (ΔE=2.7 eV) are observed in the O-1*s* NEXAFS, ~1.6 eV above transitions at 530.6 eV and 533.3 eV with identical energy separation. It is evident in Fig. 1 the O-1*s* NEXAFS spectra are quite sensitive to the incident angle (ϕ) of the x-rays; however, the transitions at 530.6 eV and 533.3 eV are present in all spectra regardless of incident angle. The features observed at 530.6 eV and 533.3 eV, as well as those at 532.2 eV and 534.9 eV, are assigned to transitions arising from oxygen anions located at the 48*f* and 8*b* sites, respectively. The constant 2.7-eV energy separation between the transitions to t_{2g} and e_g states, attributed to crystal-field splitting of TiO_6 octahedra for both 48*f* and 8*b* oxygen sites, suggests a fraction of oxygen anions from 8*b* sites are also coordinated to Ti^{4+} ions, in addition to oxygen anions from 48*f* sites. This means a fraction of Ti^{4+} ions migrate from their original 16*c* sites and displace Gd^{3+} ions from 16*d* sites. Migration of Ti^{4+} ions from their original 16*c* sites to 16*d* sites of Gd^{3+} is supported by earlier theoretical studies suggesting cation antisite disorder should be present in these pyrochlores. The 1.6-eV charge-state shift observed in the O-1*s* NEXAFS between 48*f* and 8*b* oxygen sites can be understood by considering metal-ligand bond distances and the resulting electron densities on the 48*f* and 8*b* oxygen sites. As previously mentioned, each oxygen anion in the 48*f* and 8*b* sites forms a tetrahedral coordination with two Gd^{3+} (0.254 nm) and two Ti^{4+} (0.195 nm), and four Gd^{3+} (0.221 nm) cations, respectively. The present site-sensitive O-1*s* NEXAFS data indicate a fraction of Ti^{4+} ions are also coordinated to oxygen anions from 8*b* sites following migration to 16*d* sites of Gd^{3+}. Hence, the effective electron densities on the oxygen anions should be lower for shorter Gd-O bonds (8*b*, 0.221 nm) compared to longer Gd-O bonds (48*f*, 0.254 nm). This in turn is reflected in the O-1*s* energy differences for the oxygen anions in the 48*f* and 8*b* sites, where Ti-O (48*f*) is 1.6 eV lower in energy compared to Ti-O (8*b*).

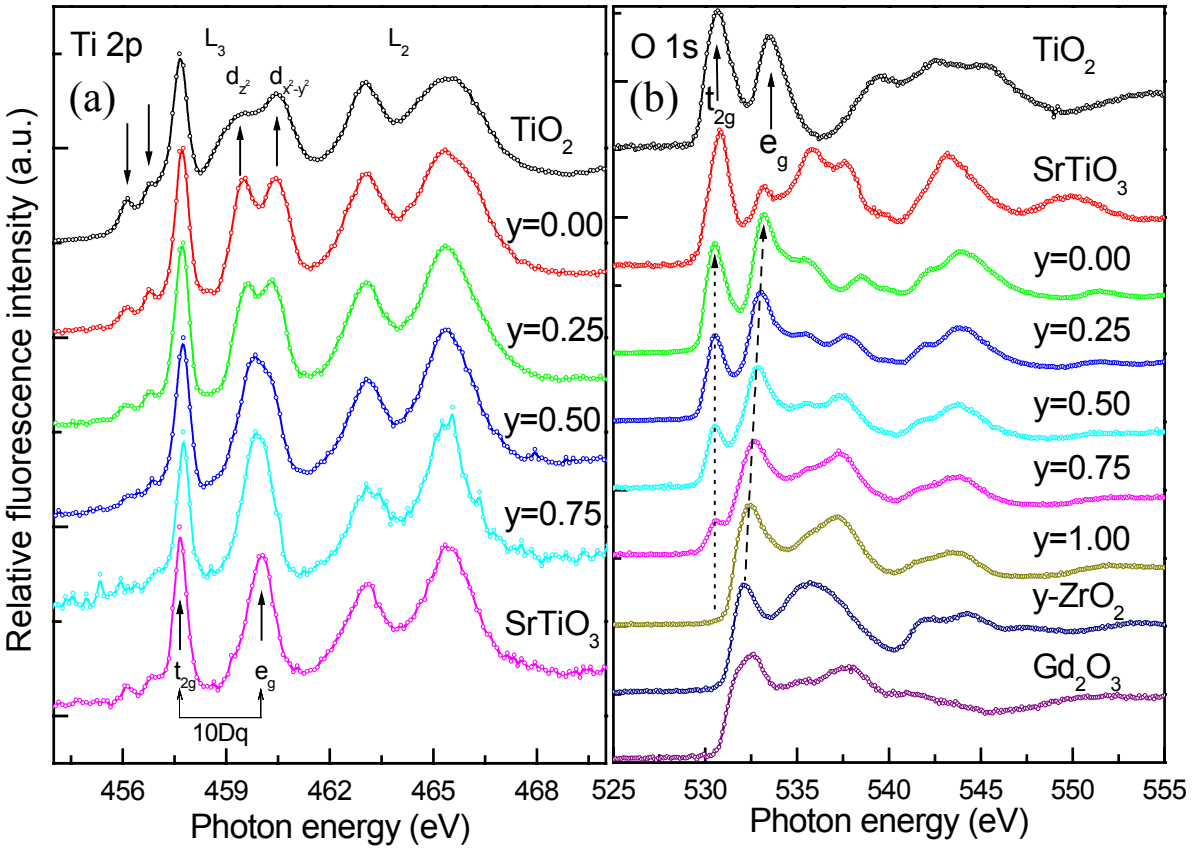

Fig. 2. (a) Titanium-2*p* NEXAFS for TiO_2 (rutile), $Gd_2(Ti_{1-y}Zr_y)_2O_7$ (y=0.0, 0.25, 0.5, and 0.75), and $SrTiO_3$. (b) Oxygen-1*s* NEXAFS for TiO_2 (rutile), $SrTiO_3$, $Gd_2(Ti_{1-y}Zr_y)_2O_7$ (y=0.0, 0.25, 0.5, 0.75, and 1.0), yttria-stabilized zirconia (y-ZrO_2), and Gd_2O_3.

The Ti-2*p* and O-1*s* NEXAFS of TiO_2 (rutile), $Gd_2(Ti_{1-y}Zr_y)_2O_7$ (y=0.0-1.0), $SrTiO_3$, yttria-stabilized zirconia (y-ZrO_2), and Gd_2O_3 are shown in Fig. 2. Although the Ti-2*p* NEXAFS show exactly the same features for both single-crystal and polycrystalline $Gd_2Ti_2O_7$, isovalent substitutions of Zr for Ti in $Gd_2Ti_2O_7$ yield significantly different spectra. The most notable observation is splitting of the e_g states, which indicates the degree of distortion from octahedral symmetry decreases with increasing Zr substitution in $Gd_2(Ti_{1-y}Zr_y)_2O_7$. Curve fitting of the transitions to the e_g states using two Gaussian functions with constant bandwidths yields energy separations between the d_{z^2} and $d_{x^2-y^2}$ orbitals, which are 1.0 eV, 0.8 eV, 0.6 eV, and 0.4 eV for $Gd_2(Ti_{1-y}Zr_y)_2O_7$, y=0.0, 0.25, 0.5, and 0.75, respectively. For TiO_2, this energy separation is 1.2 eV. In contrast, Ti in $SrTiO_3$ occupies sites with perfect octahedral symmetry, and transitions to the e_g states have no splitting, although their profiles appear slightly asymmetric. Curve fitting the transitions to the e_g states of $SrTiO_3$ yields an energy separation of ~0.5 eV which is close to that of $Gd_2(Ti_{1-y}Zr_y)_2O_7$ with y= 0.75, suggesting at this composition there is no distortion in the TiO_6 octahedra. Furthermore, the amplitude of the transitions to the e_g states relative to transitions to t_{2g} states increases with increasing Zr substitution in $Gd_2(Ti_{1-y}Zr_y)_2O_7$,

although the ratio of the integrated area under the bands and the energy separation between the t_{2g} and e_g states remain nearly constant within experimental error. These results clearly show Ti retains its octahedral symmetry, however the distortion present in TiO_6 octahedra decreases with increasing Zr substitution for Ti in $Gd_2(Ti_{1-y}Zr_y)_2O_7$.

The O-1*s* NEXAFS spectra of polycrystalline $Gd_2(Ti_{1-y}Zr_y)_2O_7$ show only transitions from oxide anions located in the 48*f* sites coordinated to both Ti^{4+} and Gd^{3+}. Thus, Gd-O also contributes spectral intensity in the vicinity of the e_g states (533.3 eV) of TiO_6 octahedra in $Gd_2Ti_2O_7$. The intensities of the transitions to t_{2g} and e_g states of the TiO_6 octahedra decrease, and the oxygen ions coordinated to Zr increasingly contribute intensity in the vicinity of transitions to e_g states in addition to those originating from Ti-O and Gd-O. This transition shifts systematically towards lower energy with increasing substitution of Zr for Ti in $Gd_2(Ti_{1-y}Zr_y)_2O_7$. Thus, a systematic shift to lower energy for the transition at 533.3 eV for y=0.0 to 532.5 eV for y=1.0 shows an increase of coordination of Zr from 6 to nearly 8 as Zr is substituted for Ti in $Gd_2(Ti_{1-y}Zr_y)_2O_7$. This is confirmed by a transition observed at 532.2 eV for yttria-stabilized zirconia (y-ZrO_2), in which Zr is situated in a cubic symmetry surrounded by eight oxygen ions. The intensity of the transition at ~532.5 eV for $Gd_2Zr_2O_7$ receives contributions from both Zr-O and Gd-O, thus the characteristics of Gd-O shift the transition ~0.3 eV to higher energy compared to the transition observed at ~532.2 eV for y-ZrO_2.

Based on crystal structure, $Ti^{4+}(Zr^{4+})$ occupies six-coordinate *B* (16*c*) sites adjacent to vacant 8*a* anion sites and forms an octahedron with oxygen anions in 48*f* sites. The O-1*s* NEXAFS show an increase in coordination of Zr from 6 to nearly 8 with increasing substitution of Zr for Ti in $Gd_2(Ti_{1-y}Zr_y)_2O_7$. Furthermore, to compensate for the increase of coordination of Zr, the vacant 8*a* anion sites adjacent to the $Ti^{4+}(Zr^{4+})$ coordination sphere need to be filled systematically. Oxygen anions, either from 48*f* or 8*b* sites, migrate to vacant 8*a* sites, giving evidence for anion disorder. The Ti in $Gd_2Ti_2O_7$ occupies octahedral sites with tetragonal distortion induced by the vacant 8*a* anion sites located in the *ab* plane of TiO_6 octahedra. In addition, the present Ti-2*p* NEXAFS show the tetragonal distortion decreases with increasing substitution of Zr for Ti in $Gd_2(Ti_{1-y}Zr_y)_2O_7$.

A phase transformation occurs from the ordered pyrochlore structure (*Fd*3*m*) to the defect fluorite structure (*Fm*3*m*) following 2.0 MeV Au^{2+} ion-beam irradiation of $Gd_2(Ti_{1-y}Zr_y)_2O_7$, irrespective of Zr concentration. Irradiated $Gd_2(Ti_{1-y}Zr_y)_2O_7$ with $y \leq 0.5$ is amorphous although there is significant short-range ordering. In contrast, compositions with $y \geq 0.75$ retain their crystallinity after ion-beam irradiation. The structures of Zr^{4+} in the irradiated $Gd_2(Ti_{1-y}Zr_y)_2O_7$ with $y \geq 0.75$ are almost the same as in cubic fluorite-structured yttria-stabilized zirconia (y-ZrO_2), providing solid evidence for the phase transformation. Rearrangements of the oxygen anions among 48*f*, 8*b*, and 8*a* sites, and of cations between the 16*c* and 16*d* sites in ordered $Gd_2Ti_2O_7$ require more energy relative to the less-ordered pyrochlore-structured $Gd_2Zr_2O_7$. Thus, during irradiation-induced phase transformation, $Gd_2(Ti_{1-y}Zr_y)_2O_7$ with $y \leq 0.5$ becomes amorphous, whereas compositions with $y \geq 0.75$ retain crystalline structure. The XPS shows a

single narrow peak at 529.6 eV with FWHM of ~1.5 eV characteristic of surface Ti-O (48*f*) in $Gd_2Ti_2O_7$.

The O-1*s* XPS of single-crystal $Gd_2Ti_2O_7$ shows a single peak at 529.6 eV with a full-width at half-maximum (FWHM) of ~1.5 eV irrespective of Ar^+-sputtering time and annealing, although there is a slight decrease in intensity in the spectra measured before annealing. The observed O-1*s* feature at 529.6 eV for $Gd_2Ti_2O_7$ is close to that of TiO_2. However, the Ti-2*p* XPS shows significant variation with Ar^+-sputtering time and annealing. The spectra recorded before annealing show Ti^{4+} reduction as a function of Ar^+-sputtering-time providing evidence sputtering removes oxygen ions from the surface of $Gd_2Ti_2O_7$, which in turn reduces the Ti^{4+} ions to lower oxidation states. The spectrum recorded after Ar^+-sputtering, followed by annealing in oxygen, shows characteristics of Ti^{4+} (as in TiO_2) indicating annealing in $2.0x10^{-6}$ Torr of O_2 at 875 K recovers the stoichiometric surface of $Gd_2Ti_2O_7$.

Waste Form Glasses

A great deal of attention is paid to speciation of radionuclide constituents in glass waste forms. However, interactions of the low-Z glass constituents actually comprising the glass network and defining its basic properties are particularly critical as well, but remain relatively under-explored. Local structural properties of glasses are not easily studied by conventional techniques because they possess no long-range order. In glass matrices, boron forms three-dimensional, rigid tetrahedral BO_4^{5-} units with sp^3 hybridization and two-dimensional, trigonally coordinated BO_3^{3-} moieties with sp^2 hybridization. The ratio of tetrahedral sp^3 to trigonal sp^2 boron strongly affects the properties of glass matrices because trigonal boron greatly reduces glass durability [5-7]. The ratio can be altered in the glass matrix by addition or removal of glass modifiers such as cations.

We have continued to investigate the effects of boron coordination by measuring and determining boron geometry in several series of glasses and reference materials. Currently, the results from our boron studies are being correlated to NMR measurements (where possible) and to leaching studies of the glasses. In particular, we have used boron *K*-edge NEXAFS to determine boron coordination for several well-known base (RD series) and Hf glass series (Hf used as a surrogate for tetravalent actinides) originating from PNNL. Boron *K*-edge NEXAFS spectra from the RD and Hf glass series are shown in Fig. 3. The ratio of tetrahedral to trigonal boron is determined by fitting the boron *K*-edge NEXAFS spectra as shown. The transition energy, the area under the band, and the ratio of tetrahedral to trigonal boron obtained are reported in Table 1. In these materials, the boron coordination varies primarily in response to changes in Na_2O, Al_2O_3, and HfO_2 content.

In a similar vein, we have continued to perform extended x-ray-absorption fine-structure (EXAFS) measurements at the sodium *K* edge from waste-form glasses and reference materials. We have finalized the data collection from two series of glasses, one the same Hf glass series mentioned above, at two temperatures along with an improved set of sodium reference materials.

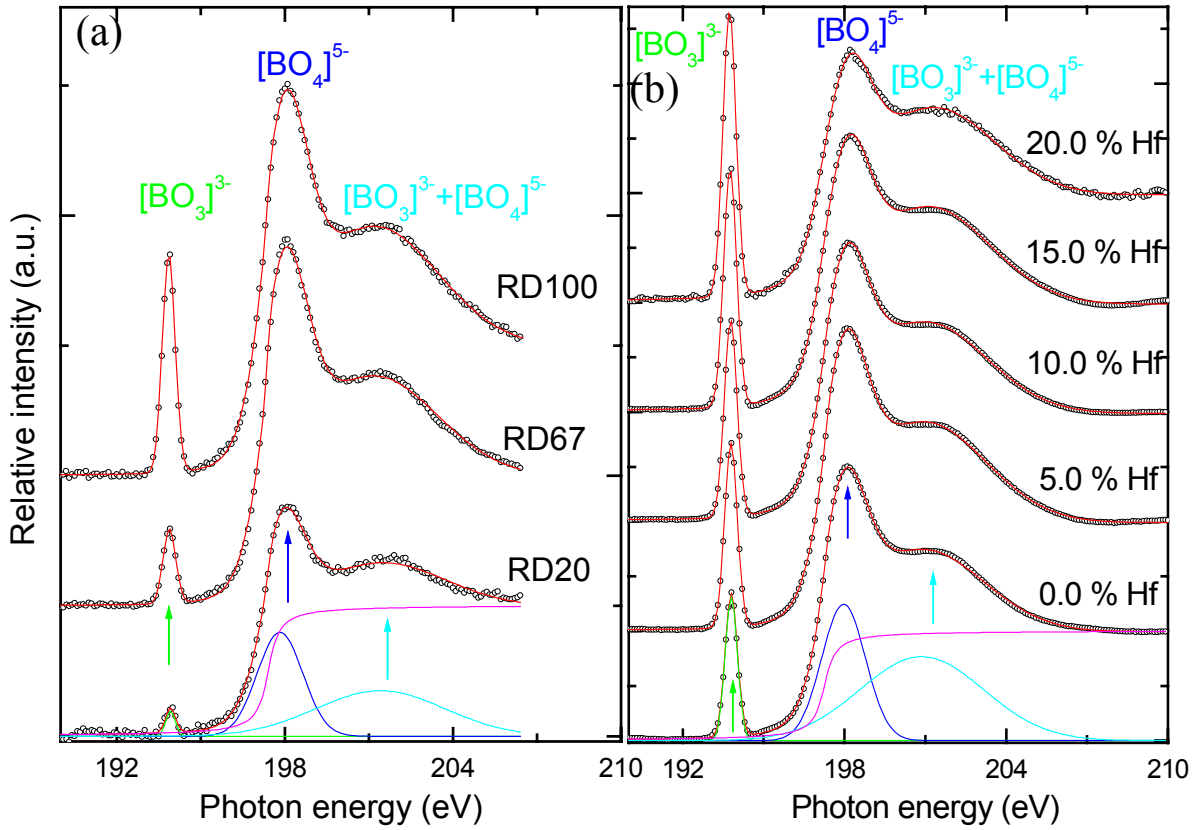

Fig. 3. Boron-1*s* NEXAFS for (a) RD and (b) Hf glass series. Curve fitting was done with three Gaussians. To fit the edge-jump, an arctangent function is also included.

Table 1. Fit results for boron *K*-edge NEXAFS for various glass samples (Peak A: $[BO_3]^{3-}$, Peak B: $[BO_4]^{5-}$, and Peak C: $[BO_3]^{3-}$ + $[BO_4]^{5-}$).

Glass	**Peak A**		**Peak B**		**Peak C**		**Tetrahedral**
	(eV)	**Area**	**(eV)**	**Area**	**(eV)**	**Area**	**Boron (B/B+A)**
00 % Hf	193.80	0.38	197.97	1.27	200.87	2.21	0.77
05 % Hf	193.79	0.49	197.99	1.47	200.93	2.70	0.75
10 % Hf	193.78	0.54	198.03	1.31	200.95	2.47	0.71
15 % Hf	193.76	0.66	198.08	1.29	201.08	2.64	0.66
20 % Hf	193.74	0.79	198.14	1.10	201.26	2.38	0.58
RD20	193.92	0.04	197.83	0.81	201.41	1.00	0.95
RD67	193.88	0.16	197.96	1.56	201.15	1.25	0.91
RD100	193.86	0.48	197.97	1.73	201.17	2.69	0.78
NaB_3Si	193.80	0.59	198.02	1.32	200.99	2.52	0.69
NaB_2Si	193.76	0.55	198.18	0.51	200.78	1.29	0.48

Inspection of the real-space EXAFS data indicates the sodium coordination in the Hf glasses exhibits no significant changes as hafnium concentration increases. Best fits were obtained when oxygen was in the first shell and silicon was in the second shell. Initially, the amplitude-reduction parameter was constrained to the value determined using the reference compounds. To check for correlation among parameters in the final fit, the amplitudes were left unconstrained and then divided by the amplitude-reduction parameter to obtain the coordination number. A mixed coordination shell of aluminum and silicon also produced a good fit to the experimental data, but the results rule out another disordered shell of oxygen, or a pure-boron or pure-aluminum shell. An initial investigation also was made on the RD series of glasses, which spans a different tieline in the base-glass phase diagram. The real-space depictions of the EXAFS (pseudo-radial distribution functions) exhibit the same general appearance and resemble the Hf-containing glasses, however there are clear differences in amplitudes and distances for several compositions.

Beamline Development

ALS Beamline 6.3.1 is an entrance-slitless bend-magnet beamline operating from 200 eV to 2000 eV with a Hettrick-Underwood type varied-line-space (VLS) grating monochromator. To meet the experimental requirements for high-performance NEXAFS of waste-form materials, rigorous developmental work has been necessary on Beamline 6.3.1 as part of this project. To eliminate experimental artifacts, spectra are normalized with the soft-x-ray photon flux measured simultaneously via a gold mesh, newly installed on the beamline. For measurement of NEXAFS spectra by surface-sensitive total-electron yield and bulk-sensitive total-fluorescence yield, respectively, a channeltron and a Hamamatsu photodiode were installed. A low-temperature sample stage also was implemented. All mirrors on the beamline were re-optimized for better flux and focused to attain higher resolution.

Summary

NEXAFS and XPS investigations have elucidated the mechanism leading to cation antisite disorder and anion Frenkel defects in $Gd_2(Ti_{1-y}Zr_y)_2O_7$ pyrochlore ceramics. These studies show Ti^{4+} ions in $Gd_2Ti_2O_7$ pyrochlore occupy octahedral sites with a tetragonal distortion induced by vacant 8*a* oxygen sites located in the *ab* plane adjacent to TiO_6 octahedra. The coordination of Zr increases from 6 to nearly 8 with increasing substitution of Zr for Ti in $Gd_2(Ti_{1-y}Zr_y)_2O_7$. To compensate for the increased coordination of Zr, oxygen anions migrate either from occupied 48*f* or 8*b* sites to vacant 8*a* sites.

A phase transformation occurs from the ordered pyrochlore structure (*Fd*3*m*) to the defect fluorite structure (*Fm*3*m*) following 2.0 MeV Au^{2+} ion-beam irradiation of $Gd_2(Ti_{1-y}Zr_y)_2O_7$, irrespective of Zr concentration. Irradiated $Gd_2(Ti_{1-y}Zr_y)_2O_7$ with $y \leq 0.5$ is amorphous although there is significant short-range ordering. In contrast, compositions with $y \geq 0.75$ retain their crystallinity after ion-beam irradiation. The structures of Zr^{4+} in the irradiated $Gd_2(Ti_{1-y}Zr_y)_2O_7$ with $y \geq 0.75$ are almost the same as cubic fluorite-structured yttria-stabilized zirconia (y-ZrO_2), providing solid evidence for phase transformation. Rearrangements of oxygen anions among the 48*f*, 8*b*, and 8*a* sites, and cations between the 16*c* and 16*d* sites in ordered $Gd_2Ti_2O_7$ require

more energy relative to the less-ordered pyrochlore-structured $Gd_2Zr_2O_7$. Thus, during phase transformation induced by ion-beam irradiation, $Gd_2(Ti_{1-y}Zr_y)_2O_7$ with $y \leq 0.5$ becomes amorphous, whereas compositions with $y \geq 0.75$ retain crystalline structure. This work has provided more information about mechanisms responsible for radiation resistance in these materials.

The ratio of tetrahedral sp^3 to trigonal sp^2 hybridized boron, which is relevant to the long-term durability of borosilicate-glass matrices, has been determined by fitting boron *K*-edge NEXAFS spectra of RD and Hf glass series. Sodium *K*-edge EXAFS was used to ascertain the local structure of sodium in the same glass series, plus others. Small differences in the local sodium arrangements were found in each series, however, the structural features did not clearly correlate with glass compositional parameters.

A complete characterization and optimization of ALS Beamline 6.3.1 was conducted to enable high-performance NEXAFS measurements of waste-form materials. The improved beamline characteristics are useful to a range of general users for a variety of scientific investigations.

Scientific Activities

Personnel on the Project and Collaborative Interactions

Dennis Lindle	UNLV, Professor of Chemistry
Ponnusamy Nachimuthu	UNLV, Postdoctoral Fellow
David Shuh	Staff Scientist, Chemical Sciences Division Lawrence Berkeley National Laboratory
David McKeown	Staff Scientist, Vitreous State Laboratory Catholic University of America
Suntharampillai Thevuthasan William J. Weber B. Pete McGrail Jonathan Icenhower	Staff Scientists Pacific Northwest National Laboratory
Rupert Perera	Staff Scientist, Center for X-ray Optics Lawrence Berkeley National Laboratory

Scientific Communications

P. Nachimuthu, Y. J. Kim, S. Thevuthasan, A. S. Lea, V. Shutthanandan, M. H. Engelhard, D. R. Baer, S. A. Chambers, D. K. Shuh, D. W. Lindle, E. M. Gullikson, and R. C. Perera, "Investigation of Copper(I) Oxide Quantum Dots by Near Edge X-ray Absorption Fine Structure Spectroscopy," submitted to Chem. Mater., October (2002).

P. Nachimuthu, S. Thevuthasan, E. M. Adams, M. H. Engelhard, B. S. Mun, W. J. Weber, D. E. McCready, B. D. Begg, D. K. Shuh, D. W. Lindle, G. Balakrishnan, D. M. Paul, E. M. Gullikson, and R. C. C. Perera, "Cation Antisite Disorder in $Gd_2Ti_2O_7$ Pyrochlore: Site-specific NEXAFS and XPS Study," in preparation for Phys. Rev. Lett., 2003

P. Nachimuthu, S. Thevuthasan, E. M. Adams, B. S. Mun, W. J. Weber, B. D. Begg, D. K. Shuh, D. W. Lindle, E. M. Gullikson, and R. C. C. Perera, "Effect of Zr Substitution for Ti in $Gd_2Ti_2O_7$ Pyrochlore: Ti 2*p* and O 1*s* NEXAFS Study," in preparation for Appl. Phys. Lett., 2003.

P. Nachimuthu, S. Thevuthasan, V. Shutthanandan, E. M. Adams, W. J. Weber, B. D. Begg, D. K. Shuh, D. W. Lindle, E. M. Gullikson, and R. C. C. Perera, "The Impact of Au^{2+} Ion Beam Irradiation on the Structural and Electronic Properties of $Gd_2(Ti_{1-y}Zr_y)_2O_7$ Pyrochlores: Ti 2*p* and O 1*s* NEXAFS Study," in preparation for J. Appl. Phys., 2003.

Presentations (from June 2002 to current date)

D. W. Lindle, "Materials Chemistry Research Program at the University of Nevada, Las Vegas," Catholic University of America, Vitreous State Laboratory, Washington, D.C. (solicited). 06 January 2002

D. K. Shuh, "Synchrotron Radiation Investigations of Actinide and Matrix Constituent Speciation in Waste Form Materials," Catholic University of America, Vitreous State Laboratory, Washington, D.C. (solicited). 06 January 2002

P. Nachimuthu, S. Thevuthasan, W. J. Weber, V. Shutthanandan, E. M. Adams, B. D. Begg, D. K. Shuh, E. M. Gullikson, D. W. Lindle, and R. C. Perera, "Characterization of Pure and Au^{2+} Irradiated $Gd_2(Ti_{1-x}Zr_x)_2O_7$ Pyrochlores by NEXAFS," Materials Research Society Fall Symposium, Boston, MA (contributed). 02-05 December 2002.

P. Nachimuthu, S. Thevuthasan, W. J. Weber, V. Shutthanandan, E. M. Adams, B. D. Begg, D. K. Shuh, D. W. Lindle, E. M. Gullikson, and R. C. C. Perera, "The Impact of Zr Substitution and Au^{2+} Ion Beam Irradiation on the Structural and Electronic Properties of $Gd_2(Ti_{1-x}Zr_x)_2O_7$ Studied by X-ray Absorption and X-ray Photoelectron Spectroscopy," Poster Presentation, ALS Users Meeting, Berkeley, CA (contributed). 10-12 October 2002.

Proposals and Reports (from June 2002 to current date)

ALS General User Proposal (ALS-00829) Renewal: P. Nachimuthu, D. W. Lindle, R. C. C. Perera, and D. K. Shuh, "Investigations of B, O, Na, and Al Speciation in Waste Form Glasses by X-ray Absorption Fine Structure Spectroscopy," (December 2002).

Acknowledgements

Parts of this work were performed in collaboration with scientists and facilities supported by other DOE programs: The Environmental Management Science Program; DOE at PNNL, which is operated by Battelle for the DOE under Contract No. DE-AC06-76RLO-1830; and the Director, Office of Science, Office of Basic Energy Sciences, Division of Chemical Sciences, Geosciences, and Biosciences of the U.S. DOE under Contract No. DE-AC03-76SF00098 at

LBNL. The NEXAFS work was conducted at the ALS, which is operated by the Director, Office of Basic Energy Sciences, U.S. DOE under Contract No. DE-AC03-76SF00098 at LBNL. The XPS work was conducted in the EMSL, a DOE user facility operated by PNNL under support from the Office of Biological and Environmental Research.

III. References

1. J. K. Bates, C. R. Bradley, E. C. Buck, J. C. Cunnane, W. L. Ebert, X. Feng, J. J. Mazer, D.J. Wronkiewicz, J. Sproull, W. L. Bourcier, B. P. McGrail, and M. K. Altenhofen, *High-Level Waste Borosilicate Glass: A Compendium of Corrosion Characteristics*, DOE-EM-0177, U.S. Department of Energy, Office of Waste Management, Washington, D.C, 1994.
2. W. J. Weber and R. C. Ewing, *Plutonium immobilization and radiation effects*, Science **289**, 2051 (2000).
3. N. J. Hess, B. D. Begg, S. D. Conradson, D. E. McCready, P. L. Gassman, and W. J. Weber, *Spectroscopic investigations of the structural phase transition in $Gd_2(Ti_{1-y}Zr_y)_2O_7$ pyrochlores*, J. Phys. Chem. B **106**, 4663 (2002).
4. J. Lian, X. T. Zu, K. V. G. Kutty, J. Chen, L. M. Wang, and R. C. Ewing, *Ion-irradiation-induced amorphization of $La_2Zr_2O_7$ pyrochlore* Phys. Rev. B. **66** 4108 (2002).
5. M. E. Fleet, and S. Muthupari, *Coordination of boron in alkali borosilicate glasses using XANES*, J. Non-Cryst. Solids **255**, 233 (1999).
6. M. E. Fleet and S. Muthupari, *Boron K-edge XANES of borate and borosilicate minerals*, Amer. Mineralogist **85**, 1009 (2000).
7. M. Kasrai, M. E. Fleet, S. Muthupari, D. Li, and G. M. Bancroft, *Surface modification study of borate materials from b k-edge x-ray absorption spectroscopy*, Phys. Chem. Minerals **25**, 268 (1998).
8. H. L. Tuller, *Solid state electrochemical systems - Opportunities for nanofabricated or nanostructured materials*, J. Electroceram. **1**, 211 (1997).
9. P. Nachimuthu, S. Thevuthasan, E. M. Adams, M. H. Engelhard, B. S. Mun, W. J. Weber, D. E. McCready, B. D. Begg, D. K. Shuh, D. W. Lindle, G. Balakrishnan, D. M. Paul, E. M. Gullikson, and R. C. C. Perera, *Cation Antisite Disorder in $Gd_2Ti_2O_7$ Pyrochlore: Site-specific NEXAFS and XPS Study*, in preparation for Phys. Rev. Letts., 2003
10. P. Nachimuthu, S. Thevuthasan, E. M. Adams, B. S. Mun, W. J. Weber, B. D. Begg, D. K. Shuh, D. W. Lindle, E. M. Gullikson, and R. C. C. Perera, *Effect of Zr Substitution for Ti in $Gd_2Ti_2O_7$ Pyrochlore: Ti 2p and O 1s NEXAFS Study*, in preparation for Appl. Phys. Letts., 2003.
11. P. Nachimuthu, S. Thevuthasan, V. Shutthanandan, E. M. Adams, W. J. Weber, B. D. Begg, D. K. Shuh, D. W. Lindle, E. M. Gullikson, and R. C. C. Perera, *The Impact of Au^{2+} Ion Beam Irradiation on the Structural and Electronic Properties of $Gd_2(Ti_{1-y}Zr_y)_2O_7$ Pyrochlores: Ti 2p and O 1s NEXAFS Study*, in preparation for J. Appl. Phys., 2003.